RYDBERG ATOMS: CORRELATIONS AND QUANTUM GATES

SUBMITTED
BY

SWETHA SRIDHAR

DIVISION OF PHYSICS & APPLIED PHYSICS
SCHOOL OF PHYSICAL AND MATHEMATICAL SCIENCES

A final year project report
presented to
Nanyang Technological University
in partial fulfilment of the
requirements for the
Bachelor of Science (Hons) in Physics / Applied Physics
Nanyang Technological University

April 2016

FYP Report

Rydberg atoms: Correlations and quantum gates

Student: Swetha Sridhar

FYP Supervisors: Asst. professor Tomasz Paterek and Assoc. professor Rainer Helmut Dumke

April 2016

Abstract

In this project, we investigate into the correlations between Rydberg atoms, excited atoms with one electron that possesses a very high principal quantum number, and the interactions that occur between them that can be used for the formation of quantum gates. We first review the fundamentals of quantum gates, followed by the nature of the interactions between Rydberg atoms and the Rydberg blockade. We study the entanglement between Rydberg atoms and the effect of the strength of dipolar interactions on the amount of generated entanglement. The crux of this study is the examination of the strong interactions between Rydberg atoms and their use in the construction of quantum gates. The final section of this report provides suggestions on future research along this direction.

Contents

1 Acknowledgements

To the higher power that placates and provides, and to my parents, for their unending patience and support. To my brother for keeping me in check.

I would like to use this opportunity to express my gratitude to Asst. Professor Tomasz Paterek and Assoc. Professor Rainer Dumke for their advice, guidance, enthusiasm and precious tidbits of knowledge. I thank Dr. Maria Valado and Tanjung Krisnanda for their invaluable time and efforts in teaching me and helping me cross hurdles through this project effortlessly. I am extremely grateful for their contributions without which this project would not be possible.

I would also like to express my gratefulness to Dr. Meng Lee Leek for his words of wisdom from my sophomore year onwards till date. His encouragement, despite all odds, has kept me going. Sincerest thanks are also due to Png Kee Seng, for his considerate and helpful nature.

To all who have been a part of my journey in Nanyang Technological University, across countries, universities and fields, thank you.

2 Introduction

Entanglement is a quantum correlation in which a quantum state cannot be assigned independently to every subsystem but can only be defined for the system as a whole. The concept of entanglement is at the heart of our understanding of quantum mechanics and serves much purpose in the study of strongly correlated systems. Entanglement between two particles can be generated by making them interact. It is difficult to produce entanglement in systems comprising of neutral atoms, as the interactions between neutral atoms are much weaker than those between ions. Here is where Rydberg atoms feature.

Rydberg atoms are neutral atoms with one electron in a state of high principal quantum number n. Due to their large size in comparison with atoms in the ground state and their high sensitivity to external fields, they form strong interatomic interactions with other Rydberg atoms. This feature of Rydberg atoms can be used to entangle neutral atoms based on the formation of the Rydberg blockade, which provides evidence for the fact that Rydberg atoms can exert a strong influence on each other even when separated by large distances that are orders of magnitude larger than the atomic size[6]. This approach has been proposed as a method to construct fast quantum gates [10][11][12] and generate various entangled states [23][24].

The unique feature of the Rydberg blockade can be used in the construction of quantum gates. If you have atoms in a small region, and you excite one of them to the Rydberg state, and then if you tried to excite another atom, the energy required would have changed due to the excitation of the first atom. This is used to turn on or turn off another atom by using a control atom.

Quantum computing is an extremely interesting research area with much promise in increasing computational power. Quantum computing also provides a platform to model quantum mechanical problems, as the modeling of such problems on a classical computer becomes hard to deal with for an extremely large number of particles.

This study aims to examine the interatomic interactions between Rydberg atoms, especially focusing on the dipole-dipole interaction. We will show the effect of strong and weak dipole-dipole interactions on generated entanglement and the probability of excitation of a detector.

Finally, the study ventures into a controlled-SWAP gate, constructed for three qubits, formed using Rydberg atoms. It reveals that controlled unitaries are relatively simple to implement via the Rydberg blockade.

3 Quantum computation

This section of the report introduces some principles of quantum computation. The power of quantum computers arises from quantum phenomena such as entanglement and the superposition of quantum states. The fundamental unit of quantum computation is a qubit, a two-level system that can be prepared and measured controllably. A quantum computer can be viewed as a collection of n qubits such that its wavefunction lies in a 2^n-dimensional complex Hilbert space. The evolution of this wavefunction in time is unitary and is governed by the Schrödinger equation.

A quantum computation is performed in the following three steps:

- Prepare of the input state
- Apply the desired unitary transformation on the input state
- Measure the output state

We now discuss the basics of quantum computation.

3.1 Two-level systems

The qubit: The qubit is the basic unit of quantum computation. It is a two-level quantum system described by a two-dimensional complex Hilbert space. The basis of a qubit is

$$|0\rangle \equiv \begin{bmatrix} 1 \\ 0 \end{bmatrix},$$

and

$$|1\rangle \equiv \begin{bmatrix} 0 \\ 1 \end{bmatrix}.$$

Any state of a qubit can be written as

$$|\psi\rangle = \alpha\,|0\rangle + \beta\,|1\rangle\,,$$

where α and β are complex and satisfy the normalization condition

$$|\alpha|^2 + |\beta|^2 = 1.$$

State vectors are defined up to a global phase that has no physical significance here. The generic state of a qubit is written as

$$|\psi\rangle = \cos\frac{\theta}{2}\,|0\rangle + e^{i\phi}\sin\frac{\theta}{2}\,|1\rangle\,.$$

$$|\psi\rangle = \begin{bmatrix} \cos\frac{\theta}{2} \\ e^{i\phi}\sin\frac{\theta}{2} \end{bmatrix}.$$

Here, $0 \leqslant \theta \leqslant \pi$ and $0 \leqslant \phi < 2\pi$. Due to this parameterization of a qubit, it can have a continuum of states. There is a geometrical representation of this state on a sphere of radius 1 called the Bloch sphere.

The Bloch sphere: The Bloch sphere is a geometric picture of a qubit. Due to the normalization condition imposed on α and β, the state of the qubit can be represented on a sphere of radius 1. The sphere can be embedded into three-dimensional space ($x = \cos\phi \sin\theta, y = \sin\phi \sin\theta, z = \cos\theta$). The state defined in the previous section can be rewritten as

$$|\psi\rangle = \begin{bmatrix} \sqrt{\frac{1+z}{2}} \\ \frac{x+iy}{\sqrt{2(1+z)}} \end{bmatrix}.$$

A Bloch vector is a vector whose components mark a point on the Bloch sphere. Each Bloch vector satisfies the condition $x^2 + y^2 + z^2 = 1$. Angles θ and ϕ also define a Bloch vector, as shown in the figure below 1.

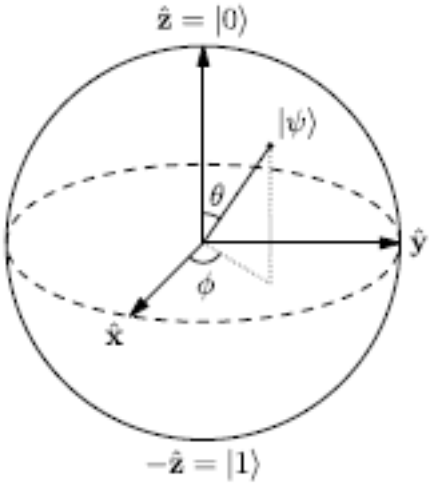

Figure 1: The Bloch sphere is a geometric representation of a qubit. The state can be defined by the angles θ and ϕ on a sphere of radius 1. Figure obtained from [9].

Measurement of the state of a qubit: An arbitrary observable with ± 1 outcomes can be parameterized by a unit vector similar to the parameterization of quantum states. We shall now show how the coordinates of a qubit state can be measured. For that, we would need the Pauli operators, written in the computational basis as follows:

$$X = \sigma_x = \begin{bmatrix} 0 & 1 \\ 1 & 0 \end{bmatrix},$$

$$Y = \sigma_y = \begin{bmatrix} 0 & -i \\ i & 0 \end{bmatrix},$$

and

$$Z = \sigma_z = \begin{bmatrix} 1 & 0 \\ 0 & -1 \end{bmatrix}.$$

Applying these on $|\psi\rangle = \cos\frac{\theta}{2}|0\rangle + e^{i\phi}\sin\frac{\theta}{2}|1\rangle$,

$$\sigma_x|\psi\rangle = e^{i\phi}\sin\frac{\theta}{2}|0\rangle + \cos\frac{\theta}{2}|1\rangle,$$

$$\sigma_y|\psi\rangle = -ie^{i\phi}\sin\frac{\theta}{2}|0\rangle + i\cos\frac{\theta}{2}|1\rangle,$$

and

$$\sigma_z|\psi\rangle = \cos\frac{\theta}{2}|0\rangle - e^{i\phi}\sin\frac{\theta}{2}|1\rangle.$$

The expectation values for the state are

$$\langle\psi|\sigma_x|\psi\rangle = \sin\theta\cos\phi = x,$$

$$\langle\psi|\sigma_y|\psi\rangle = \sin\theta\sin\phi = y,$$

and

$$\langle\psi|\sigma_z|\psi\rangle = \cos\theta = z.$$

Therefore, (x, y, z) can be obtained by measurements of σ_x, σ_y and σ_z respectively.

3.2 Single-qubit gates

The operations on a qubit are defined by $2x2$ unitary matrices, as they must preserve the normalization condition. This section will introduce two single-qubit gates: the Hadamard gate and the phase-shift gate.

The Hadamard gate: This gate is defined as

$$H = \frac{1}{\sqrt{2}}\begin{bmatrix} 1 & 1 \\ 1 & -1 \end{bmatrix},$$

and it turns the computational basis $|0\rangle, |1\rangle$ into the new basis $|+\rangle, |-\rangle$, the states of which are a superposition of the states of the computational basis:

$$H|0\rangle = \frac{1}{\sqrt{2}}(|0\rangle + |1\rangle) \equiv |+\rangle$$

$$H|1\rangle = \frac{1}{\sqrt{2}}(|0\rangle - |1\rangle) \equiv |-\rangle$$

The phase-shift gate: This gate is defined as

$$R_z(\delta) = \begin{bmatrix} 1 & 0 \\ 0 & e^{i\delta} \end{bmatrix},$$

and it turns $|0\rangle$ to $|0\rangle$ and $|1\rangle$ to $e^{i\delta}|1\rangle$. Global phases have no physical meaning and therefore, the states of the computational basis remain unchanged. The action of the phase-shift gate on a single qubit is given by

$$R_z(\delta)|\psi\rangle = \begin{bmatrix} 1 & 0 \\ 0 & e^{i\delta} \end{bmatrix} \begin{bmatrix} \cos\frac{\theta}{2} \\ e^{i\phi}\sin\frac{\theta}{2} \end{bmatrix} = \begin{bmatrix} \cos\frac{\theta}{2} \\ e^{i(\phi+\delta)}\sin\frac{\theta}{2} \end{bmatrix},$$

and this generates a counterclockwise rotation about z through an angle δ on the Bloch sphere.
Any unitary operation on a single qubit can be constructed using only the above two gates [7].

3.3 Entanglement generation and controlled gates

Entanglement appears in the presence of two qubits. A generic two-qubit state can be expressed in the computational basis as

$$|\psi\rangle = \alpha|00\rangle + \beta|01\rangle + \gamma|10\rangle + \delta|11\rangle,$$

where, α, β, γ and δ are complex coefficients that obey the normalization condition

$$|\alpha|^2 + |\beta|^2 + |\gamma|^2 + |\delta|^2 = 1.$$

This state is defined up to an overall phase factor, and there are six degrees of freedom. In general, it is not possible to consider $|\psi\rangle$ as a separable state.
A state $|\psi\rangle$ is separable when one can write $|\psi\rangle$ as

$$|\psi\rangle = |\psi_1\rangle \otimes |\psi_0\rangle,$$

where $|\psi_1\rangle$ and $|\psi_0\rangle$ are the wavefunctions of the two subsystems of the state. A separable state comprising of two qubits has four degrees of freedom, obtained by considering two parameters for each qubit on the Bloch sphere.
A single-qubit state, as defined in 3.2, cannot generate entanglement in an n-qubit system. This is because, if we were to consider a separable state

$$|\psi\rangle = |\psi_{n-1}\rangle \otimes |\psi_{n-2}\rangle \otimes ... \otimes |\psi_0\rangle,$$

any qubit can be moved on its Bloch sphere, giving

$$|\psi'\rangle = |\psi'_{n-1}\rangle \otimes |\psi'_{n-2}\rangle \otimes ... \otimes |\psi'_0\rangle,$$

where any state of the type $|\psi_j\rangle$ can be transformed by single-qubit gates acting on the j^{th} qubit in any superposition of the states $|0\rangle$ and $|1\rangle$, but the n-qubit state is still separable.
Therefore, in order to prepare an entangled state, there is a need for inter-qubit interactions through two-qubit gates. A two-qubit gate that can generate entanglement is the controlled-NOT gate or the CNOT gate. The working of this gate is elucidated in section 3.4.

The Bell basis: From 3.4, we can see that CNOT gates can generate entanglement. The entangled states of the Bell basis, given by

$$|\phi^+\rangle = \frac{1}{\sqrt{2}}(|00\rangle + |11\rangle),$$
$$|\phi^-\rangle = \frac{1}{\sqrt{2}}(|00\rangle - |11\rangle),$$
$$|\psi^+\rangle = \frac{1}{\sqrt{2}}(|01\rangle + |10\rangle),$$
$$|\psi^+\rangle = \frac{1}{\sqrt{2}}(|01\rangle - |10\rangle),$$

can be obtained from the computational basis by the following transformations

$$|00\rangle \to |\phi^+\rangle\,,$$
$$|01\rangle \to |\psi^+\rangle\,,$$
$$|10\rangle \to |\phi^-\rangle\,,$$
$$|11\rangle \to |\psi^-\rangle\,,$$

which is invertible as both the Hadamard gate and the CNOT gate are self-inverse. As a result of this, any state of the Bell basis can be transformed into a separable state.

3.4 Quantum gates

Any unitary operation in the Hilbert space of n qubits can be decomposed into single-qubit gates and two-qubit CNOT gates [7]. This section elaborates upon two two-qubit gates that will be used later in the report.

SWAP gate: A SWAP gate is a two-input two-output gate that swaps the logical values of the states entered. Figure 2 gives the truth values of the SWAP gate. The gate is represented in circuit diagrams as in the figure 3.

a	b	a'	b'
0	0	0	0
0	1	1	0
1	0	0	1
1	1	1	1

Figure 2: Truth table for the SWAP gate.

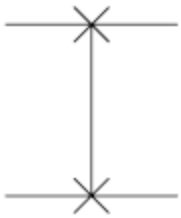

Figure 3: Circuit representation for the SWAP gate. Here a and b are the inputs. a' and b' are the outputs.

CNOT gate: A CNOT gate is a controlled-NOT gate, in which one atom acts as the control, while the other undergoes the NOT operation. If the control atom has the logical value of 0, the second atom does not change its truth value. Figure 4 gives the truth values of the CNOT gate. The gate is represented in circuit diagrams as in the figure 5.

a	b	a'	b'
0	0	0	0
0	1	0	1
1	0	1	1
1	1	1	0

Figure 4: Truth table for CNOT gate.

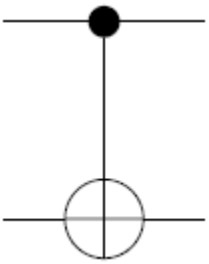

Figure 5: Circuit representation for the CNOT gate. Here a and b are the inputs. a' and b' are the outputs.

As mentioned in 3.3, the CNOT gate is a two-qubit gate that can generate entanglement.
In the CNOT gate, the first qubit acts as the control and the second as the target. This gate flips the state of the target atom if the state of the control atom is $|1\rangle$ and does nothing if the state of the control is $|0\rangle$.

The matrix representation of the CNOT gate is as follows:

$$\begin{bmatrix} 1 & 0 & 0 & 0 \\ 0 & 1 & 0 & 0 \\ 0 & 0 & 0 & 1 \\ 0 & 0 & 1 & 0 \end{bmatrix}.$$

Taking the square of the above matrix, one can conclude that the CNOT gate is self-inverse.

We can generate entangled states using the CNOT gate as follows:

$$CNOT(\alpha\,|0\rangle + \beta\,|1\rangle)\,|0\rangle = \alpha\,|00\rangle + \beta\,|11\rangle\,,$$

which is a non-separable state, provided $\alpha, \beta \neq 0$.

4 Rydberg atoms

Rydberg atoms are atoms that are excited to a high energy state and have one electron in a state of high principal quantum number n. The focus was shifted onto them in the 1970s, but their role in atomic physics can be traced back to the infancy of quantitative atomic spectroscopy, as described by H. E. White in his text on *Introduction to Atomic Spectra* published in 1934. The first historic appearance of Rydberg atoms is in the Balmer series of atomic Hydrogen, and is given by

$$\lambda = \frac{bn^2}{n^2 - 4},$$

where λ gives the wavelength, b is $3645.6\mathring{A}$ and $n = 2$ to higher levels for the Balmer series.
J. R. Rydberg generalized the above expression for each pair of states n_1 and n_2, such that the energy difference between the two states is as follows:

$$W_2 - W_1 = \frac{k^2 Z^2 e^4 m}{2\hbar^2}\left(\frac{1}{n_1^2} - \frac{1}{n_2^2}\right),$$

where e is the charge of the electron, m is the mass of the electron, k is $\frac{1}{4\pi\varepsilon_0}$ and Z is the atomic number. $\frac{k^2 Z^2 e^4 m}{2\hbar^2} = Ry$, where Ry is the Rydberg constant, given by $109721.6cm^{-1}$. The expression for the wavelength thus obtained is:

$$\frac{1}{\lambda} = Ry\left(\frac{1}{n_1^2} - \frac{1}{n_2^2}\right).$$

Compared to ground state atoms, Rydberg atoms exhibit large sizes. For example, for a Rubidium (Rb) in the ground state ($5S$), the orbit radius is $5.632a_0$. If now, we compare this with a Rb atom in the Rydberg state ($43S$) whose orbit radius is $2384.2a_0$ [4]. Their orbit radius is given by

$$\langle r \rangle = \frac{1}{2}(3(n^*)^2 - l(l+1)),$$

where l is the angular quantum number and n^* is the effective quantum number given by $n^* = n - \delta_{n,l,j}$[1], the details of which can be found in section 4.1. From the above formula, one can conclude that the size of Rydberg atoms is proportional to n^2.
Rydberg atoms are characterized by an electron in a high energy state with principal quantum number n. Due to this, the properties of Rydberg atoms are highly "exaggerated". For instance, the binding energy of Rydberg atoms, which is of the order of $300GHz$ for $n = 100S$, is very small. Binding energy is given by

$$E = \frac{e^2}{a_0}\frac{m - m_e}{m}\frac{1}{2(n - \delta_{n,l,j})^2},$$

where $e^2 = \frac{q_e^2}{4\pi\varepsilon_0}$, m_e is the mass of the electron, m is the mass of the atom, q_e is the electronic charge, a_0 is the Bohr radius and ε_0 is the permittivity of free space. $n^* = n - \delta_{n,l,j}$ is the effective quantum number 4.1 where $\delta_{n,l,j}$ is the quantum defect that mainly depends on the orbital angular momentum l of the outermost

electron. The orbits of the low l angular states are the most perturbed with large quantum defect 4.1 [13]. The radiative lifetime of Rydberg atoms is very long in atomic scale, in the order of several μs. For example, the lifetime of Rydberg atoms, that is determined by the radiative decay to lower levels and by transitions to higher and lower lying levels induced by blackbody radiation, is of the order of 100 or so μs for $n \geqslant 40$, which is much larger than the lifetime of the $5P_{\frac{3}{2}}$, which is approximately $26.2ns$[4].

The radial dipole matrix elements are big and are of the order of $a_0 n^2$. The electric dipole transition matrix can have huge values of the order of $n^2 q_e a_0$, where the atomic unit of the electric dipole moment is $-q_e a_0 = 8.48x10^{-}30C.m$ [13]. 4.4

Rydberg states are very sensitive to even modest electric fields. Their high sensitivity is due to their large size and loose binding to the electron core. They are readily polarized and even ionized in relatively weak electric fields. This property will be looked into further in section 4.2.

4.1 The quantum defect

Despite the shielding of the valence electrons from the electric field of the nucleus, there is a quantum defect, the cause for which is embedded in the fact that Rydberg atoms do not have circular orbits [1]. The quantum defect has been determined by spectroscopy, and can be approximated using the formula below:

$$\delta_{n,l,j} = \delta_0 + \frac{\delta_2}{(n-\delta_0)^2} + \frac{\delta_4}{(n-\delta_0)^4} + ...$$

and the values of δ_0, δ_2 and so on are determined experimentally for the atomic species under consideration. Quantum Defect Theory quantifies the deviations of the core potential of the species considered from that of the standard hydrogen model. The energy eigenvalues undergo a correction obtained by replacing the principal quantum number n by an effective quantum number n^*, described as $n^* = n - \delta_{n,l,j}$[1].

Now that the effective quantum number has been defined, various other properties can be expressed based on the scaling of n^* as in the table 1.

4.2 Rydberg atoms in an electric field

Rydberg atoms are highly sensitive to electric fields, producing what is called the Stark effect. Ground state atoms are nearly unaffected by external electric fields, but the Rydberg energy levels are easily perturbed and even ionized by electric fields. This effect can be better comprehended through the following:

Consider a perturbation due to an applied electric field F along the z axis: $V = ezF$. Applying perturbation theory to the second order, one can obtain the energy eigenvalues to be approximately

$$E_n = E_n^0 + \langle n^{(0)} | V | n^{(0)} \rangle + \sum_{k \neq n} \frac{| \langle n^{(0)} | V | k \rangle |^2}{E_n^0 - E_k^0}.$$

Property	n^***-scaling**
Binding energy E_n	$(n^*)^{-2}$
Orbital radius	$(n^*)^2$
Level spacing	$(n^*)^{-3}$
Lifetime τ	$(n^*)^3$
Ionisation field ε_{ion}	$(n^*)^{-4}$
Dipole-dipole interaction coefficient C_3	$(n^*)^4$
van der Waals interaction coefficient C_6	$(n^*)^{11}$
Polarizability α	$(n^*)^7$

Table 1: Some general properties of Rydberg atoms and their scaling laws with respect to the effective quantum number n^*

For low values of angular momentum, the energy levels are not degenerate, and the quadratic Stark shift term is the dominant term

$$\Delta E = \sum_{k \neq n} \frac{|\langle n^{(0)}| V |k\rangle|^2}{E_n^0 - E_k^0} = \frac{1}{2}\alpha F^2,$$

where α is the polarizability. Electric polarizability is the tendency of a charge distribution to be distorted by an external electric field or by an ion or dipole in close proximity. The scaling for α can be obtained from table 1.

In the case of Rb, the polarizability of the $5S$ ground state is $\alpha = -79.4 MHzV^2cm^{-2}$, whilst the polarizability of the $43S$ Rydberg state is $\alpha = -17.7 MHzV^2cm^{-2}$, which shifts this state, at an external field of $1Vcm^{-1}$, 350 linewidths to the red [4] on the Stark map, where the linewidth of Rb transition $5S \rightarrow 6P$ is approximately $60MHz$.

4.3 Electric dipole moment

Due to the large size of the Rydberg atom, the valence electron is separated from the core by a large distance. This leads to a large electric dipole moment $\vec{\mu}$. They are easily polarized by external electric fields.

The electric dipole moment $\vec{\mu}$ of an atom is given by

$$\vec{\mu} = -a_0 e < \vec{r} >,$$

where a_0 is the Bohr radius, $-e$ is the electronic charge and $\vec{r}$ is the separation of the valence electron from the core, the expectation value of which is 0 for pure angular momentum states.

4.4 Interactions between Rydberg atoms

Due to their extreme sensitivity, Rydberg atoms readily interact with other Rydberg atoms separated even by large distances of the order of several μm. They are governed by two types of interactions-Dipole-dipole interactions and van der Waals interactions. This section ventures into these interactions and also deals with an interesting feature of Rydberg atoms, namely, the Rydberg blockade. Dipole-dipole interactions are extremely strong, and will be used later in this study.

4.4.1 Dipole-dipole and van der Waals interactions

Dipole-dipole interactions are interatomic interactions that have a short range and are dependent on the orientation of the dipoles. van der Waals interactions are interatomic interactions that have a wider range and are relatively independent of orientation, making them ubiquitous in nature. Consider an electrostatic dipole with dipole moment μ generating an electric field that can be described as:

$$\vec{E}(\vec{r}) = \frac{1}{4\pi\varepsilon_0}\frac{3(\vec{n}\cdot\vec{\mu})\vec{n}-\vec{\mu}}{R^3},$$

where $\vec{R} = R\vec{n}$.

The dipole-dipole interaction between two atoms separated by $\vec{R}$ is given by

$$V_{dd} = \frac{1}{4\pi\varepsilon_0}\frac{\vec{\mu}_1\cdot\vec{\mu}_2 - 3(\vec{\mu}_1\cdot\vec{n})(\vec{\mu}_2\cdot\vec{n})}{R^3}.$$

Here, μ_1 and μ_2 are the electric dipole moments of atoms 1 and 2 respectively. If one were to apply a small

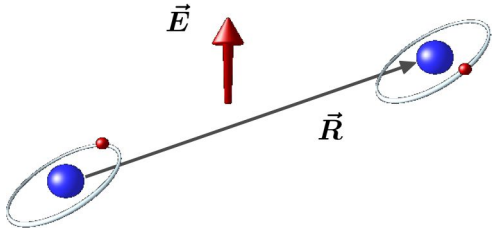

Figure 6: Two dipole-dipole interacting Rydberg atoms placed in a weak electric field $\vec{E}$.

electric field $\vec{F}$, a given state $|r\rangle$ is coupled only with the state closest in energy to it $|r'\rangle$, describing the Hamiltonian in this case as

$$\begin{bmatrix} E_r & \frac{\vec{\mu_1}\vec{\mu_2}}{R^3} \\ \frac{\vec{\mu_1}\vec{\mu_2}}{R^3} & E_r + \Delta_F \end{bmatrix}.$$

Here, E_r correspond to the energies of the state $|r\rangle$. Δ_F is the Förster defect that is the quantifier of the energy difference between two pairs of states and the value gives the different types of interactions. The eigenvalues of this Hamiltonian are

$$E_\pm = \frac{\Delta_F}{2} \pm \sqrt{\left(\frac{\Delta_F}{2}\right)^2 + \left(\frac{\mu_1\mu_2}{R^3}\right)^2}.$$

Dipole-dipole interactions at resonance: These interactions occur at small distances or at Förster resonance ($\Delta_F = 0$). In this case, the dipole-dipole term dominates ($\frac{\mu_1\mu_2}{R^3} >> \Delta_F$) and the energy shift is given by

$$\Delta E = \pm\frac{\hbar C_3}{R^3}.$$

The scaling for C_3 can be obtained from the table 1.

van der Waals interaction: These interactions occur at larger distances ($\frac{\mu_1\mu_2}{R^3} << \Delta_F$) and the energy shift is given by

$$\Delta E = \pm\frac{\hbar C_6}{R^6}.$$

The scaling for C_6 can also be obtained from the table 1.

4.5 Angular dependence of the dipole-dipole interaction

The angular dependence of the dipole-dipole interaction makes it a characteristic of the interaction. This can be controlled externally in order to vary the strength of the interaction between the two dipoles.
Consider the expression for the dipole-dipole interaction defined earlier:

$$V_{dd} = \frac{1}{4\pi\varepsilon_0}\frac{\vec{\mu}_1\cdot\vec{\mu}_2 - 3(\vec{\mu}_1\cdot\vec{n})(\vec{\mu}_2\cdot\vec{n})}{R^3}.$$

Here, the separation between the two atoms, whose dipole moments are $\vec{\mu_1}$ and $\vec{\mu_2}$, is given by $\vec{R} = R\vec{n}$. Also, the dipole moments are given by $\vec{\mu_1} = e\vec{r_1}$ and $\vec{\mu_2} = e\vec{r_2}$. The following is the derivation for the angular dependence of V_{dd}. For simplicity, we neglect $\frac{1}{4\pi\varepsilon_0}$ in the derivation, as it does not affect the results thus obtained.
Factoring out e^2,

$$V_{dd} = \frac{e^2}{R^3}(\vec{r}_1\cdot\vec{r}_2 - 3(\vec{r}_1\cdot\vec{n})(\vec{r}_2\cdot\vec{n})).$$

Now, the matrix elements for the interaction are calculated by

$$\langle\psi_1|\langle\psi_2|V_{dd}|\psi_2'\rangle|\psi_1'\rangle = \frac{e^2}{R^3}\langle\psi_1|\langle\psi_2|(\vec{r}_1\cdot\vec{r}_2 - 3(\vec{r}_1\cdot\vec{n})(\vec{r}_2\cdot\vec{n}))|\psi_2'\rangle|\psi_1'\rangle,$$

where $|\psi_1\rangle$ and $|\psi_2\rangle$ are the initial states and $|\psi_1'\rangle$ and $|\psi_2'\rangle$ are the final states.
Writing the scalar products explicitly,

$$\langle\psi_1|\langle\psi_2|V_{dd}|\psi_2'\rangle|\psi_1'\rangle = \frac{e^2}{R^3}\langle\psi_1|\langle\psi_2|(x_1x_2+y_1y_2+z_1z_2-3(x_1\hat{n}_x+y_1\hat{n}_y+z_1\hat{n}_z)(x_2\hat{n}_x+y_2\hat{n}_y+z_2\hat{n}_z))|\psi_2'\rangle|\psi_1'\rangle,$$

where

$$\hat{n}_x = \sin\theta\cos\phi\hat{x},$$

$$\hat{n}_y = \sin\theta\sin\phi\hat{y},$$

and

$$\hat{n}_z = \cos\theta\hat{z}.$$

We do not consider the radial component here. Substituting the components of $\vec{n}$ into the matrix element and then averaging over ϕ, we obtain three types of angular dependence:

$$f_1 = (1 - 3\cos^2\theta)^2,$$

$$f_2 = 9\sin^2\theta\cos^2\theta,$$

and

$$f_3 = 9\sin^4\theta.$$

f_1 is the angular dependence expected when two dipoles are aligned. This corresponds to a resonant energy exchange between states, where $\Delta m_j = 0$ for both atoms or where $\Delta m_j = \pm 1$ for one atom and $\Delta m_j = \mp 1$ for the other atom. Here, m_j is the z component of the total angular momentum [14].
f_2 corresponds to $\Delta m_j = 0$ for one atom and $\Delta m_j = \pm 1$ for the other atom and f_3 corresponds to $\Delta m_j = \pm 1$ for both atoms [14].

There is the aspect of the alignment of the dipole moments of the atoms with respect to the applied external field $\vec{F}$, as shown in figure 7.

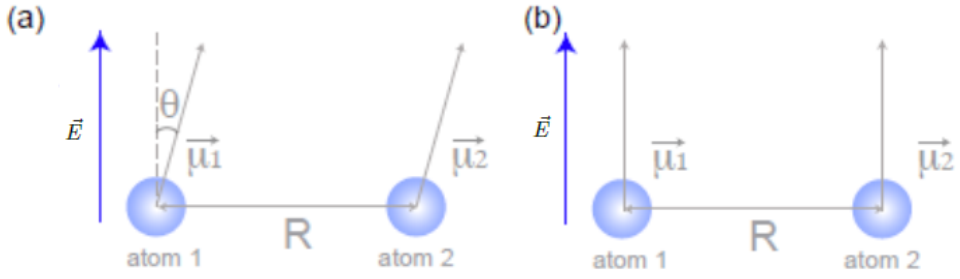

Figure 7: *a)* shows two excited atoms that are separated by a distance R in the presence of an external electric field $\vec{E}$ with an angle θ between the electric field vector and the dipole moment of an atom $\vec{\mu_1}$. *b)* shows the dipole moments $\vec{\mu_1}$ and $\vec{\mu_2}$ in alignment with the direction of the electric field $\vec{E}$. Figure adapted from [8].

4.6 The Rydberg blockade

A direct consequence of the strong dipole-dipole interactions is the formation of the Rydberg blockade. The excitation of a particular atom can be suppressed by a neighbouring atom that has been excited to the

Rydberg state.

When a laser is shone on a cloud, some atoms are excited to their Rydberg states, which creates a blockade sphere with radius

$$r_b = \sqrt[6]{\frac{C_6}{\hbar\Omega}},$$

where Ω is the Rabi frequency. From 8, we can understand the effect of the Rydberg blockade. When the

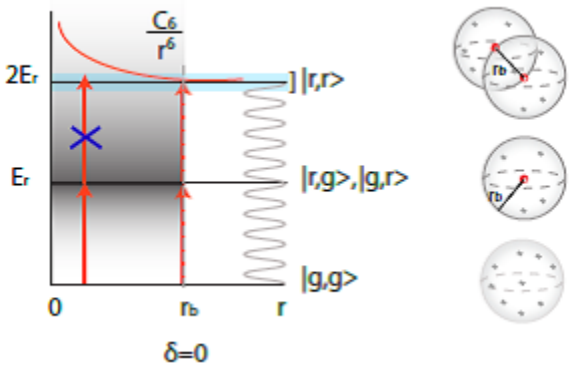

Figure 8: The figure is a schematic representation of the dipole blockade. Once an atom is excited to its Rydberg state, the interactions between the Rydberg atoms cause a shift of the energy levels of the surrounding ground state atoms within a sphere defined by the radius of influence r_b, thus blocking their excitation. Figure obtained from [8].

applied laser field is resonant with the excitation frequency of a single Rydberg atom, a second Rydberg atom in the vicinity of the first atom cannot be excited due to a shift in energy, which leaves the second atom off-resonant with the field.

4.7 Relevance of the Rydberg blockade to quantum gates

Neutral atoms have state dependent interaction properties and weak coupling with field noises, which makes them essential in the implementation of two-qubit quantum gates [10]. To put it differently, the lack of a strong Coulomb interaction in neutral atoms leads to much lesser coupling with stray fields than in the case of ions. However, Rydberg atoms can be used to implement quantum gates by taking advantage of the strong dipole-dipole interactions that Rydberg atoms possess. From the figure 9, the dependence of the two-particle interaction strength on the separation R is evident for ions, neutral atoms in the ground state and Rydberg atoms (Rubidium atoms in the $100s$ level). From 9, the interaction of Rydberg atoms is governed by van der Waals forces in the long range and dipole-dipole interactions in the short range. The former is scaled as $\frac{1}{R^6}$ and the latter as $\frac{1}{R^3}$. Two-atom interactions for Rydberg atoms can be switched on and off with a gap

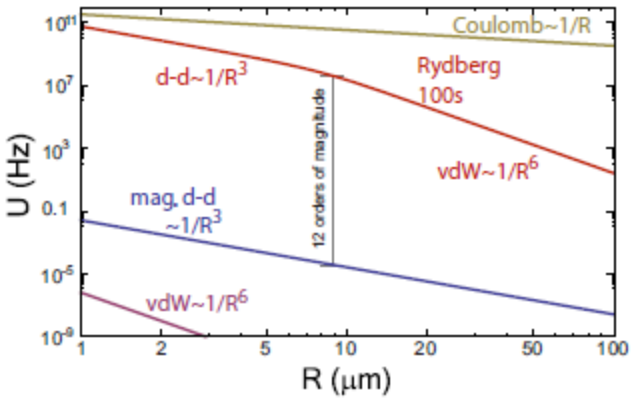

Figure 9: Two-body interaction strength for Rubidium atoms in the ground state, Rubidium atoms excited to the $100S$ level and ions (Coulombic interaction). Figure obtained from [10].

of 12 orders of magnitude, establishing control over a wide range and thus making Rydberg atoms ideal for quantum computing. The feature of the Rydberg blockade has been proposed as an application to implement quantum gates in neutral gases [12]. The challenge in the case of quantum gates is to be able to isolate quantum information from environmental decoherence as well as to allow for strong, controllable interactions between qubits. In the figure 10, there are two atoms under consideration-the control and the target. If

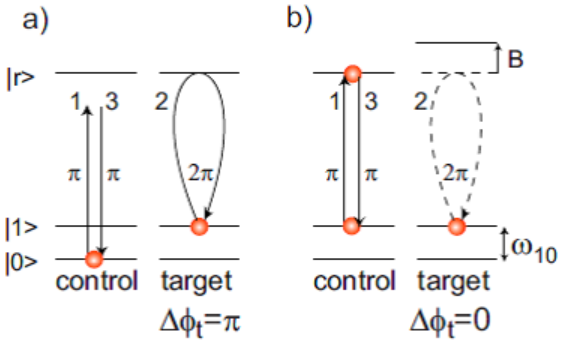

Figure 10: A phase gate controlled by the Rydberg blockade. The Rydberg blockade controlled phase gate operates on states $|01\rangle$ and $|10\rangle$ in a) and b) respectively. Information is stored in the basis states $|0\rangle$ and $|1\rangle$. State $|1\rangle$ is coupled to the Rydberg level $|r\rangle$ with excitation Rabi frequency Ω. The controlled phase gate is implemented by a three pulse sequence. a) is when the control atom starts at $|0\rangle$ and is not excited to $|r\rangle$, so there is no blockade formed. b) is when the control atom is in $|1\rangle$, which is excited to $|r\rangle$, leading to the formation of the blockade. Figure obtained from [10].

the control atom is Rydberg excited with a resonant laser pulse, the target atom is excited and becomes

off-resonant and is thus blocked. The reason for this is the dipole-dipole interactions formed between the two Rydberg atoms. The figure has a Rydberg blockade controlled phase gate that operates on two input states $|01\rangle$ and $|11\rangle$, the former being a) and the latter, b). Information is stored in $|0\rangle$ and $|1\rangle$. $|1\rangle$ is coupled with the Rydberg level $|r\rangle$ with Rabi frequency Ω. A three-pulse sequence regulates the controlled phase gate:

$$\pi : |1\rangle \rightarrow |r\rangle \, control \tag{1}$$

$$2\pi : |1\rangle \rightarrow |r\rangle \rightarrow |1\rangle \, target \tag{2}$$

$$\pi : |r\rangle \rightarrow |1\rangle \, control \tag{3}$$

In a), the control atom is at $|0\rangle$ initially, implying that it is not Rydberg excited and preventing the formation of a blockade. In b), the control atom is at $|1\rangle$, which is Rydberg excited, leading to the formation of the Rydberg blockade. The evolution matrix of the above is a controlled-Z gate, that can be transformed into a controlled-NOT (CNOT) gate by adding $\frac{\pi}{2}$ rotations between $|0\rangle \rightarrow |1\rangle$ on the target atom both before and after interaction. The CNOT gate coupled with single qubit operations, such as the Hadamard gates and phase gates, form the set of universal gates [9]. Extending the above to ensemble qubits consisting of N atoms each [11], one can see that the Rydberg blockade can block the excitation of a large number of atoms.

Development of the CNOT gate: A neutral atom can be used to control a NOT gate. An implementation of the CNOT gate comprises of single qubit rotations using two photon stimulated Raman pulses [19], a coherent excitation of Rydberg states and the formation of the Rydberg blockade. Consider a system of two atoms, in which one is the control atom and the other is the target. The excitation and subsequent de-excitation of the target atom corresponds to a 2π rotation of the effective spin which leads to a phase shift to the wavefunction of the target. If the control atom and target atom form a blockade such that the control atom is in the Rydberg level and the target atom is blocked from excitation, then no such rotation occurs and there is no phase shift of the wavefunction of the target. This is a C_Z controlled phase operation. One can convert the Rydberg blockade to CNOT gates in many ways. It is possible to perform Hadamard rotations on the target before and after the controlled phase [19], generating an $H - C_z$ CNOT. One can also implement an AS-CNOT (controlled amplitude SWAP), as shown in the figure 11. In the figure 11 (the figure on the right), when the control atom is in $|0\rangle$, it is excited to its Rydberg level by pulse 1 and thus the blockade is formed, preventing pulses 2, 4 and 6 from having any effect on the target atom. Pulse 7 returns the atom to $|0\rangle$. In the figure on the left, in which the control atom is at $|1\rangle$, pulses 1 and 7 are detuned, and pulses $2 - 6$ swap the amplitudes of $|1\rangle$ and $|0\rangle$. On the right, when the control is at $|0\rangle$, the switch is turned off and on the left, the switch is turned on, causing the NOT operation to occur.
Figure 12 provides a schematic for the CNOT gate, which can be realized experimentally.

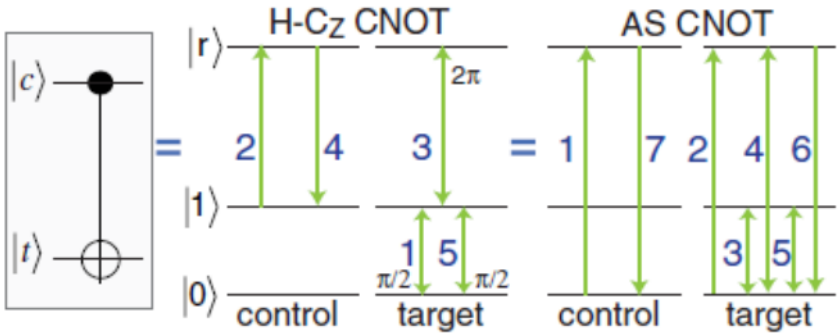

Figure 11: CNOT gates with Hadamard rotations. The pulses are all π pulses unless mentioned otherwise. When the control atom is in $|0\rangle$, as in the figure on the right, it is excited to its Rydberg level by pulse 1 and thus the blockade is formed, preventing pulses 2, 4 and 6 from having any effect on the target atom. Pulse 7 returns the atom to $|0\rangle$. In the figure on the left, in which the control atom is at $|1\rangle$, pulses 1 and 7 are detuned, and pulses $2-6$ swap the amplitudes of $|1\rangle$ and $|0\rangle$. On the right, when the control is at $|0\rangle$, the switch is turned off and on the left, when the control is at $|1\rangle$, the switch is turned on. Figure obtained from [19].

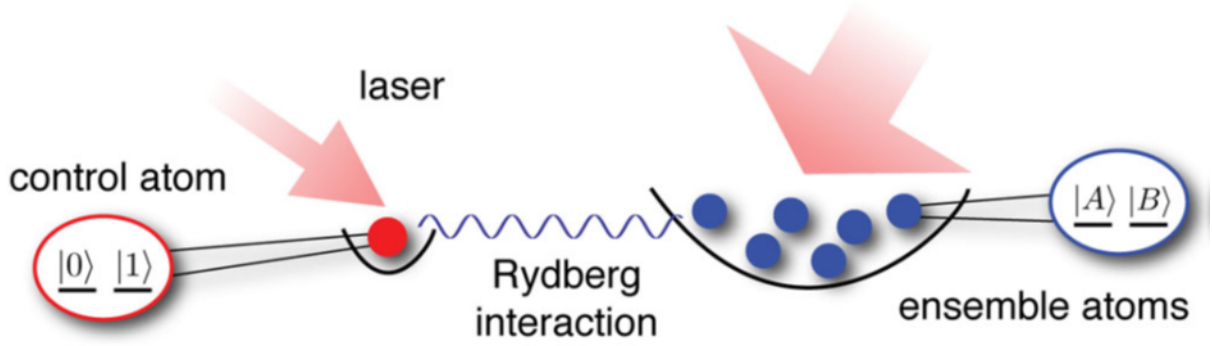

Figure 12: An atomic ensemble in its quantum state, manipulated by a single control atom and the Rydberg interaction. Figure obtained from [24].

5 Results and discussions

5.1 System of two Rydberg atoms

The $\vec{\mu}\cdot\vec{E}$ interaction between a light field and an atom can be treated to be the same all over the atom due to the minute size of the electron compared to the wavelength of the field. Here, $\vec{\mu}$ is the electric dipole moment and $\vec{E}$ is the electric field. $\vec{\mu} \propto \hat{r}$, as the size of the electric dipole is distance times charge. An approximation is made that the electric field is monochromatic and a plane wave. A description of the electric field can be

given as below:

$$\vec{E}(r) = i\vec{\epsilon}E_0[ae^{i\vec{k}\vec{r}} - a^\dagger e^{-i\vec{k}\vec{r}}].$$

Here, $k = \frac{\omega}{c}$ is the wavenumber, E_0 is the field strength, r is the position of the desired field, $\vec{\epsilon}$ is the polarization and a and $a^\dagger$ are the creation and annihilation operators for photons in the mode. The Hamiltonian for the evolution of the field is

$$H_{field} = \hbar\omega a^\dagger a,$$

which is consistent with the notion that the energy is the volume integral of $|\vec{E}|^2$ in the cavity.

The two-level atom approximation can be employed here because we are only dealing with monochromatic light and only relevant energy levels that satisfy the two following conditions:

- The energy difference of the energy levels matches the energy of the incident photons, and
- Selection rules do not inhibit transitions.

From energy conservation,

$$\hbar\omega = E_2 - E_1,$$

where E_1 and E_2 are the two eigenenergies of the atom. Conservation of angular momentum and parity are accounted for by considering the matrix elements of $\hat{r}$ between two orbital wavefunctions $\langle l_1, m_1| \hat{r} |l_2, m_2\rangle$. One can take $\hat{r}$ in the $\hat{x} - \hat{y}$ plane and express it in spherical harmonics

$$\hat{r} = \sqrt{\frac{3}{8\pi}}[(-r_x + ir_y)Y_{1,+1} + (r_x + ir_y)Y_{1,-1}].$$

Here, l_1, l_2, m_1 and m_2 are the quantum numbers, $|m| \leqslant l$. $Y_{l,m}$ are the spherical harmonics.
The relevant terms in $\langle l, m_1| \hat{r} |l, m_2\rangle$ in this basis are

$$\int Y^*_{l,m_1} Y_{1,m} Y_{l_z,m_z} d\Omega.$$

Applying selection rules, the above integral is non-zero only when $m_2 - m_1 = \pm 1$ and $\Delta l = \pm 1$. Under the dipole approximation, where $\langle l_1, m_1| \hat{r} |l_2, m_2\rangle$ becomes relevant, the former condition is the conservation of angular momentum and the latter, conservation of parity. The reason for the use of this approximation is the simplicity it offers. If $|\psi_1\rangle$ and $|\psi_2\rangle$ are two levels, then the matrix elements of $\hat{r}$ are

$$r_{ij} = \langle\psi_i| \hat{r} |\psi_j\rangle \approx r_0 Y,$$

where r_0 is a constant and Y is a Pauli operator. The Hamiltonian of the atom in this two-level subspace is

$$H_{atom} = \frac{\hbar\omega_0}{2} Z,$$

where $\hbar\omega_0$ is the energy difference between the two levels as they are both energy eigenstates. Using the quantum mechanical approximation of the electric field with creation and annihilation operators, and the matrix elements of $\hat{r}$ in the two-level approximation, the interaction Hamiltonian is

$$H_I = -igY(a - a^\dagger).$$

We have chosen $r = 0$ to place the atom and orient it in such a way that $\hat{r}$ is aligned with $\vec{E}$. g is a constant that describes the strength of the interaction. H_I is Hermitian and can be simplified using the Pauli raising and lowering operators below

$$\sigma_\pm = \frac{1}{2}(X \pm iY).$$

H_I is then given as

$$H_I = g(\sigma_+ - \sigma_-)(a - a^\dagger).$$

The cross-terms with $\sigma_+ a^\dagger$ and $\sigma_- a$ oscillate at twice the values of ω and ω_0, and can hence be dropped by the rotating wave approximation. The total Hamiltonian is

$$H = \frac{\hbar\omega_0}{2}Z + \hbar\omega a^\dagger a + g(a^\dagger\sigma_- + a\sigma_+),$$

which is $H = H_{atom} + H_{field} + H_I$. ω is the frequency of the field and ω_0 is the frequency of the atom. g is the coupling constant for the interaction between the field and the atom. Using $N = a^\dagger a + \frac{Z}{2}$ and the fact that $[H, N] = 0$, where N is the constant of motion, the Hamiltonian can be rewritten as

$$H = \hbar\omega N + \delta Z + g(a^\dagger\sigma_- + a\sigma_+),$$

where δ is the detuning given by

$$\delta = \frac{\omega_0 - \omega}{2}.$$

Now we shall delve into Rabi oscillations, that are a characteristic of field-atom systems.

Rabi oscillations of a system: Consider two identical Rydberg atoms A and B. First, we examined the results of shining a laser of frequency Ω on one of the atoms, say A. The same result was obtained when the laser was shone on B. The Hamiltonian for a single atom on which a laser is shone is

$$H = -\begin{bmatrix} \delta & 0 & 0 \\ 0 & \delta & g \\ 0 & g & -\delta \end{bmatrix}.$$

Here, g is the coupling constant and δ is the detuning, i.e., the frequency difference between the field and atomic resonance.The basis states are $|00\rangle, |01\rangle, |10\rangle$. The time evolution is given by the unitary operator

$$U = e^{-iHt}.$$

N can be neglected as it contributes a fixed phase only, and $\hbar$ is dropped for convenience. Using the above, we can determine that

$$U = e^{-i\delta t} |00\rangle \langle 00| + (\cos\Omega t + i\frac{\delta}{\Omega}\sin\Omega t) |01\rangle \langle 01| + \cos\Omega t - i\frac{\delta}{\Omega}\sin\Omega t) |10\rangle \langle 10| - i\frac{g}{\Omega}\sin\Omega t(|01\rangle \langle 10| + |10\rangle \langle 01|).$$

The fourth term gives that the field and the atom oscillate, exchanging energy at the Rabi frequency

$$\Omega = \sqrt{g^2 + \delta^2}.$$

Coming back to our system, the laser was first shone on one atom and then on the other separately. Then, the laser was shone on the system. As the two atoms in consideration are Rydberg atoms, they will interact with each other with the dipole-dipole interaction described previously 4.4. The construction of the system is as in figure 13. When the laser is shone on one atom, we obtain Rabi oscillations that look like in figure

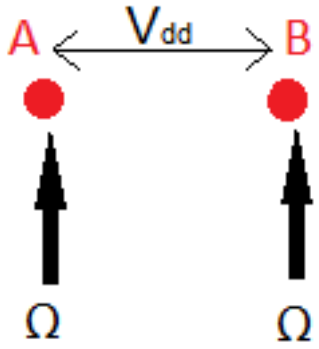

Figure 13: This is a system of two Rydberg atoms A and B that interact with V_{dd} between them. A laser of frequency Ω is shone on both A and B.

14. The figure was obtained by considering the Hamiltonian for a single atom irradiated by a laser.
When the system is irradiated by two lasers, the above can be divided into two cases, based on the strength of the dipole-dipole interactions: weak interactions and strong interactions. Consider the following Hamiltonian for the system of two atoms, A and B:

$$H = \frac{\hbar\Omega}{2}(|0\rangle \langle 1| + |1\rangle \langle 0|) \otimes \mathbb{1}_B - \hbar\Delta({\sigma_z}^A \otimes \mathbb{1}_B) + \frac{\hbar\Omega}{2}\mathbb{1}_A \otimes (|0\rangle \langle 1| + |1\rangle \langle 0|) - \hbar\Delta(\mathbb{1}_A \otimes {\sigma_z}^B) + V_{dd} |1\rangle \langle 1| \otimes |1\rangle \langle 1|.$$

Here, Ω is the Rabi frequency, $\mathbb{1}$ represents the identity matrix, $\Delta\sigma_z$ is the detuning and V_{dd} is the dipole-dipole potential. The Hamiltonian for this system was obtained by

$$H = H_A + H_B + H_{interaction},$$

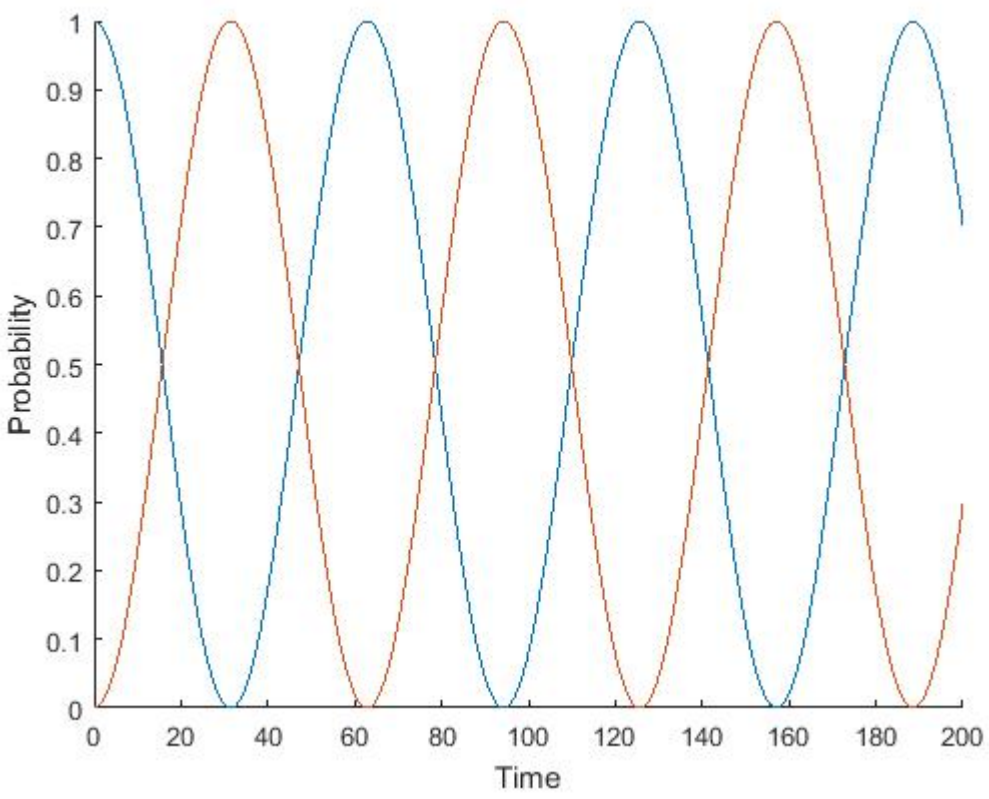

Figure 14: Rabi oscillations obtained for a single atom in a system of two Rydberg atoms. The laser is shone only on one atom. Note that the time has been made dimensionless. The blue graph depicts the oscillation of the ground state, and the red graph depicts the oscillation of the excited state. Time is given by $x = \omega t$.

where H_A is the Hamiltonian for A, H_B is the Hamiltonian for B and $H_{interaction}$ is obtained by evaluating the dipole-dipole interaction. Consider atom A in this system.

$$H_A = E_0 \left|0\right\rangle \left\langle 0\right| + E_1 \left|1\right\rangle \left\langle 1\right|,$$

where E_0 and E_1 are the energy eigenvalues such that $E_1 - E_0 = \delta$ and $E_1 + E_0 = S$. Therefore, $2E_1 = \delta + S$ and $2E_0 = S - \delta$. Substituting for E_1 and E_0 in H_A,

$$H_A = \frac{S-\delta}{2} \left|0\right\rangle \left\langle 0\right| + \frac{S+\delta}{2} \left|1\right\rangle \left\langle 1\right|,$$

which can be simplified to

$$H_A = \frac{S}{2}(\left|0\right\rangle \left\langle 0\right| + \left|1\right\rangle \left\langle 1\right|) - \frac{\delta}{2}(\left|0\right\rangle \left\langle 0\right| - \left|1\right\rangle \left\langle 1\right|),$$

which is,

$$H_A = \frac{S}{2}\mathbb{1} - \frac{\delta}{2}\sigma_z,$$

where $\mathbb{1}$ is the identity matrix, defined as $|0\rangle\langle 0| + |1\rangle\langle 1|$ and σ_z is the Pauli Z matrix, given by $|0\rangle\langle 0| - |1\rangle\langle 1|$. The same calculation can be repeated for atom B.

The interaction Hamiltonian, as mentioned earlier, is obtained from the dipole-dipole interaction between A and B. The dipole-dipole interaction can be described as

$$V_{dd} = \frac{1}{4\pi\varepsilon_0}\frac{\vec{\mu}_1 \cdot \vec{\mu}_2 - 3(\vec{\mu}_1 \cdot \vec{n})(\vec{\mu}_2 \cdot \vec{n})}{R^3},$$

where ε_0 is the permittivity of free space, $\vec{\mu_1}$ is the dipole moment of A, $\vec{\mu_2}$ is the dipole moment of B and the interaction between two atoms in an applied electric field separated by a distance R is measured along $\vec{n}$. The matrix of V_{dd} in the basis $|gg\rangle, |gr\rangle, |rg\rangle, |rr\rangle$, where the first term gives the state of$A$ and the second of B, is as follows:

$$V_{dd} = \begin{bmatrix} 0 & \delta & \delta & d_1 d_2 \\ \delta & 0 & \delta & d_1 \mu_2 \\ \delta & \delta & 0 & \mu_1 d_2 \\ d_1 d_2 & d_1 \mu_2 & \mu_1 d_2 & \mu_1 \mu_2 \end{bmatrix}.$$

However, the value of δ is very small. Terms $d_L d_R, d_L \mu_R, \mu_L d_R$ are extremely small and are also neglected. The only term that remains in V_{dd} is the one obtained by $\langle rr| V_{dd} |rr\rangle$. Therefore,

$$V_{dd} = \begin{bmatrix} 0 & 0 & 0 & 0 \\ 0 & 0 & 0 & 0 \\ 0 & 0 & 0 & 0 \\ 0 & 0 & 0 & \mu_1 \mu_2 \end{bmatrix}.$$

In order to plot the graphs, some dimensionless parameters were introduced.

$$\frac{\Omega}{\omega} = e,$$

$$\frac{\Delta}{\omega} = d,$$

and

$$\frac{V_{dd}}{\hbar\omega} = v.$$

This made the Hamiltonian purely numerical.

So where exactly does ω come from? We consider the Hamiltonian

$$H = \frac{\hbar\Omega}{2}(|0\rangle\langle 1| + |1\rangle\langle 0|) \otimes \mathbb{1}_B - \hbar\Delta({\sigma_z}^A \otimes \mathbb{1}_B) + \frac{\hbar\Omega}{2}\mathbb{1}_A \otimes (|0\rangle\langle 1| + |1\rangle\langle 0|) - \hbar\Delta(\mathbb{1}_A \otimes {\sigma_z}^B) + V_{dd} |1\rangle\langle 1| \otimes |1\rangle\langle 1|,$$

which can be rewritten using the Pauli matrices as

$$H = \frac{\hbar\Omega}{2}(\sigma_x^A \otimes \mathbb{1}_B) - \hbar\Delta({\sigma_z}^A \otimes \mathbb{1}_B) + \frac{\hbar\Omega}{2}(\mathbb{1}_A \otimes \sigma_x^B) - \hbar\Delta(\mathbb{1}_A \otimes {\sigma_z}^B) + V_{dd} |1\rangle\langle 1| \otimes |1\rangle\langle 1|.$$

We then factor out $\hbar$ and multiply and divide by ω, which has the same dimensions as Ω.

$$H = \hbar\omega\left(\frac{1}{2}\frac{\Omega}{\omega}(\sigma_x^A \otimes \mathbb{1}_B) - \frac{\Delta}{\omega}(\sigma_z{}^A \otimes \mathbb{1}_B) + \frac{1}{2}\frac{\Omega}{\omega}(\mathbb{1}_A \otimes \sigma_x^B) - \frac{\Delta}{\omega}(\mathbb{1}_A \otimes \sigma_z{}^B) + \frac{V_{dd}}{\hbar\omega}\left|1\right\rangle\left\langle 1\right| \otimes \left|1\right\rangle\left\langle 1\right|\right).$$

This can be written as

$$H = \hbar\omega H_0,$$

where

$$H_0 = \frac{1}{2}\frac{\Omega}{\omega}(\sigma_x^A \otimes \mathbb{1}_B) - \frac{\Delta}{\omega}(\sigma_z{}^A \otimes \mathbb{1}_B) + \frac{1}{2}\frac{\Omega}{\omega}(\mathbb{1}_A \otimes \sigma_x^B) - \frac{\Delta}{\omega}(\mathbb{1}_A \otimes \sigma_z{}^B) + \frac{V_{dd}}{\hbar\omega}\left|1\right\rangle\left\langle 1\right| \otimes \left|1\right\rangle\left\langle 1\right|.$$

In order to evolve the state with respect to time, a numerical approximation was considered like so

$$\left|\psi(t)\right\rangle = e^{-\frac{iHt}{\hbar}}\left|\psi(0)\right\rangle,$$

which, when approximated, becomes

$$\left|\psi(t)\right\rangle = \lim_{n\to\infty}\left(\mathbb{1} - \frac{iH\Delta t}{\hbar}\right)^n\left|\psi(0)\right\rangle,$$

where $\Delta t = \frac{t}{n}$. Also,

$$e^{-\frac{iHt}{\hbar}} = e^{-\frac{iH_0\hbar\omega t}{\hbar}} = e^{-iH_0\omega t} = e^{-iH_0 x},$$

where $x = \omega t$.

The initial state is

$$\left|\psi(0)\right\rangle = \left|00\right\rangle = \left|0\right\rangle \otimes \left|0\right\rangle = \begin{bmatrix} 1 \\ 0 \end{bmatrix} \otimes \begin{bmatrix} 1 \\ 0 \end{bmatrix},$$

thus giving

$$\left|\psi(0)\right\rangle = \begin{bmatrix} 1 \\ 0 \\ 0 \\ 0 \end{bmatrix}.$$

When the laser is shone on the system, there are two cases for V_{dd}: strong interactions and weak interactions. For strong interactions, the ratio of V_{dd} to Ω is

$$\frac{V_{dd}}{\Omega} >> 1,$$

and for weak V_{dd},

$$\frac{V_{dd}}{\Omega} << 1,$$

where Ω is the Rabi frequency.

In the case of strong V_{dd}, we obtain an oscillation of the state below:

$$|\psi_+\rangle = \frac{1}{\sqrt{2}}(|01\rangle + |10\rangle),$$

where the first term gives the state of A and the second of B. The frequency of oscillation in this case is given by $\sqrt{2}\Omega$.

In the case of weak V_{dd}, the oscillations obtained are very slow. To illustrate this, we plot a negativity versus time graph. This is an indicator of the time taken to achieve maximum entanglement for both strong and weak dipole-dipole interactions.

Negativity: The non-separability of states is given by negative eigenvalues of the matrix obtained by the partial transposition of the density matrix. The absolute value of the negative values is a measure of entanglement for general states and is known as negativity [5]. The maximum possible value of negativity is 0.5. It is defined as

$$\mathcal{N}_{A-B} = \frac{||\rho^{T_A}||_1 - 1}{2},$$

where $||\rho^{T_A}||_1$ is the trace norm of the density matrix, calculated after a partial transposition with respect to A.

The trace norm of $||\rho||_1$ of a matrix ρ is the sum of the singular values of ρ, given by the roots of the eigenvalues of $\rho\rho^\dagger$. Therefore,

$$||\rho||_1 = Tr\sqrt{\rho\rho^\dagger}.$$

From the figure 15, for strong V_{dd}, maximum entanglement is reached at $\approx 2.2 \times 10^3$ unit time. From the figure 16, for weak V_{dd}, maximum entanglement is reached at $\approx 6.2 \times 10^4$ unit time. From this, we can conclude that, in the case of weak interactions, entanglement grows much slower and maximum entanglement is attained much later than in the case of strong interactions. The ratio of the time to achieve maximum entanglement in the case of weak V_{dd} over strong V_{dd} is approximately $10:1$.

In figure 15, upon close observation, one can notice that the graph does not touch zero. This is because of an imperfect blockade. Also, in figure 16, a wiggle is observed in the oscillation. This wiggle is actually the graph of negativity for the strong V_{dd} tilted and 'fitted' along the graph of negativity for weak V_{dd}.

In the instances in which probability was calculated, the following method was used: The density matrix of a given state $|\psi_+\rangle$ is given by

$$P(|\psi_+\rangle) = |\psi_+\rangle \langle\psi_+|,$$

This implies that, if we were to obtain the probability of finding a particle in the state ϕ, we calculate the integral $\langle\phi|\rho|\phi\rangle$. The trace of ρ is normalized to 1 and the trace of ρ^2 is 1 for pure states and < 1 for mixed states.

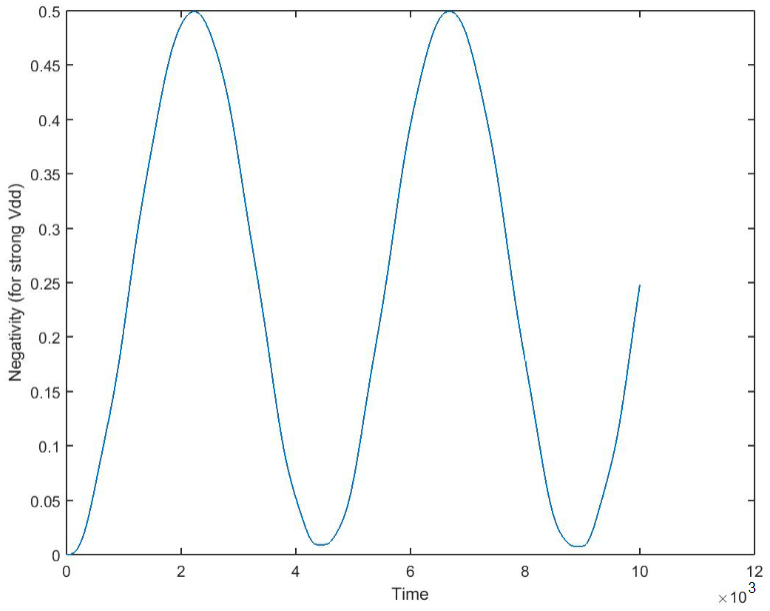

Figure 15: Negativity versus time graph in the case of strong V_{dd} between A and B. Time is given by x, where $x = \omega t$.

Say we have the following state:

$$|\psi\rangle = \frac{1}{8}|00\rangle + \frac{1}{4}|01\rangle + \frac{3}{8}|10\rangle + \frac{1}{4}|11\rangle .$$

We must calculate the probability of $|00\rangle$. We can determine this by

$$\langle 00|\,\rho\,|00\rangle = \langle 00|\left(\frac{1}{8}|00\rangle\langle 00| + \frac{1}{4}|01\rangle\langle 01| + \frac{3}{8}|10\rangle\langle 10| + \frac{1}{4}|11\rangle\langle 11|\right)|00\rangle .$$

Due to the orthonormality of the basis vectors,

$$\langle 00|\,\rho\,|00\rangle = \langle 00|\left(\frac{1}{8}|00\rangle\langle 00|\right)|00\rangle ,$$

which gives

$$\langle 00|\,\rho\,|00\rangle = \frac{1}{8}.$$

5.2 System of three Rydberg atoms

Consider three Rydberg atoms A, B and C such that A and B are entangled, and atom C acts as a probe, which detects $A - B$. C interacts only with A. A laser was shone on C alone and the interaction between A and C was examined. We recorded graphs for strong and weak V_{dd} between A and C for C. We start with $A - B$ in state

$$|\psi\rangle = \frac{1}{2}(|01\rangle + |10\rangle),$$

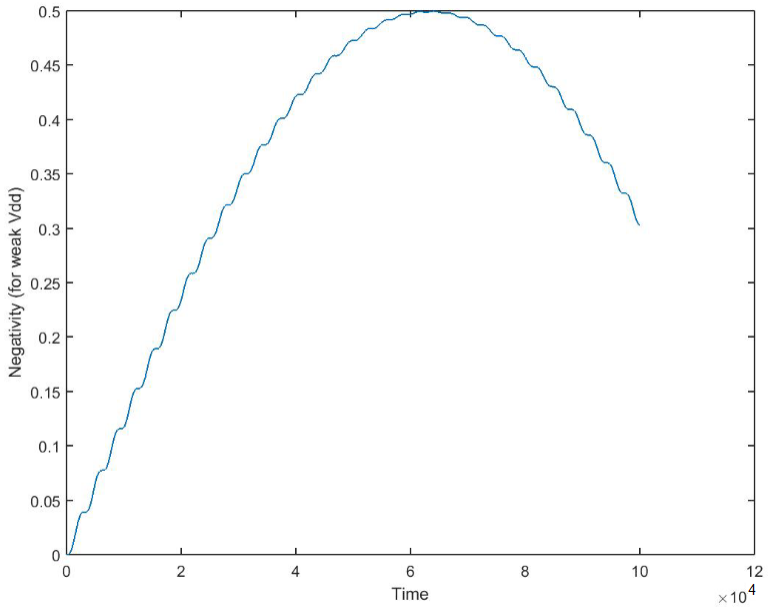

Figure 16: Negativity versus time graph in the case of weak V_{dd} between A and B. Time is given by x, where $x = \omega t$.

and C in state $|0\rangle$.

After A and C have interacted, we separate A and B far apart to study the interaction between A and C. If the interaction between them is weak, we obtain Rabi oscillations for C, as in figure 17. If the interaction between them is strong, we obtain the figure 18.

The state of C, in the case of strong V_{dd}, evolves from $|0\rangle$ to

$$|\psi\rangle = osc\,|C\rangle\,\frac{1}{\sqrt{2}}\,|01\rangle + noosc\,|C\rangle\,\frac{1}{\sqrt{2}}\,|10\rangle\,,$$

where *osc* implies oscillation and *noosc* implies no oscillation.

To obtain the graphs 17 and 18, the following calculations were made:

In the case of weak V_{dd},

$$P(|0\rangle) = \cos^2\frac{\Omega t}{2},$$
$$P(|1\rangle) = \sin^2\frac{\Omega t}{2}.$$

This gives Rabi oscillations as in figure 17.

In the case of strong V_{dd},

$$\rho_{ABC} = |\psi\rangle\,\langle\psi|\,,$$

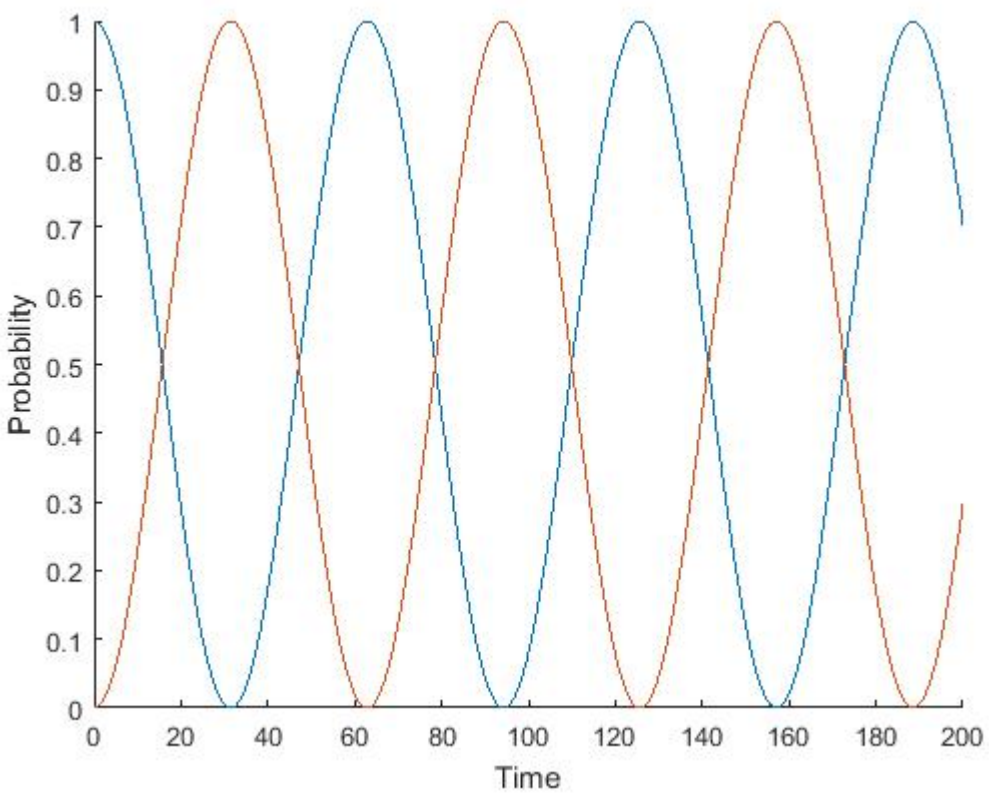

Figure 17: Rabi oscillations for C in a system in which an entangled system $A-B$ interacts with a probe C. A and B are separated and the interaction between A and C was studied. The above is the result for weak V_{dd} interaction between A and C. Time is given by $x = \omega t$. The blue graph depicts the oscillation of the ground state, and the red graph depicts the oscillation of the excited state.

where ρ_{ABC} is the density matrix. The state $|\psi\rangle$ is

$$|\psi\rangle = \frac{1}{\sqrt{2}}\left(\cos\frac{\Omega t}{2}|0\rangle + \sin\frac{\Omega t}{2}|1\rangle\right).$$

The probabilities thus obtained are

$$P(|0\rangle) = tr(|0\rangle\langle 0|\,\rho_A) = \frac{1}{2}\left(\cos^2\frac{\Omega t}{2} + 1\right),$$

and

$$P(|1\rangle) = tr(|1\rangle\langle 1|\,\rho_A) = \frac{1}{2}\left(\sin^2\frac{\Omega t}{2}\right),$$

where $\rho_A = tr_{BC}(\rho_{ABC})$. This gives the result obtained in figure 18.

We will compare the probabilities obtained above in a special case, in which $\frac{\Omega t}{2} = \frac{\pi}{2}$. In the case of weak V_{dd},

$$P(|0\rangle) = \cos^2\frac{\Omega t}{2} = 0,$$

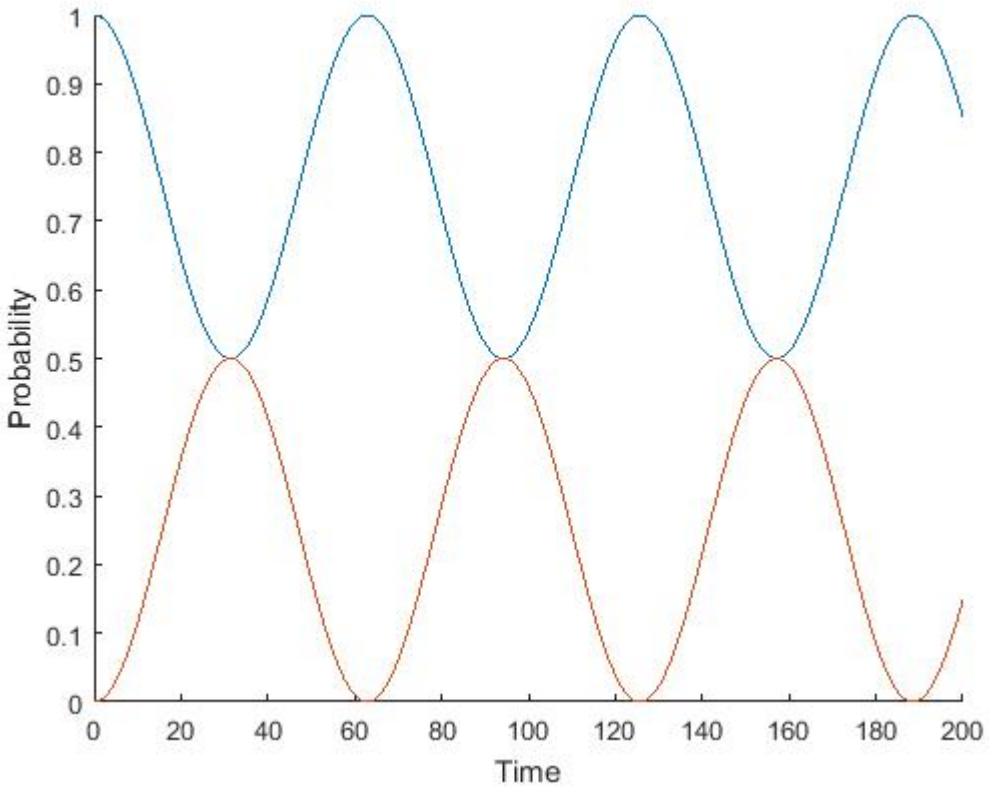

Figure 18: The above is the result for strong V_{dd} interaction between A and C. Time is given by $x = \omega t$. The blue graph depicts the oscillation of the ground state, and the red graph depicts the oscillation of the excited state.

$$P(|1\rangle) = \sin^2 \frac{\Omega t}{2} = 1,$$

and, in the case of strong V_{dd},

$$P(|0\rangle) = tr(|0\rangle \langle 0| \rho_A) = \frac{1}{2}\left(\cos^2 \frac{\Omega t}{2} + 1 \right) = \frac{1}{2},$$

and

$$P(|1\rangle) = tr(|1\rangle \langle 1| \rho_A) = \frac{1}{2}\left(\sin^2 \frac{\Omega t}{2} \right) = \frac{1}{2}.$$

From the above, we can conclude that measurements destroy entanglement.

5.3 Development of the controlled-SWAP gate

Consider three atoms A, B and C. C is the control atom, based on which the SWAP operation takes place between A and B. When the truth value of C is 0, the SWAP operation does not take place. When the

truth value of C is 1, the SWAP operation occurs and A and B switch values. The truth table for this operation for all 8 possible combinations is given in table 2. The operation that this gate performs can be

A	B	C	A'	B'	C'
0	0	0	0	0	0
1	0	0	1	0	0
0	1	0	0	1	0
1	1	0	1	1	0
0	0	1	0	0	1
1	0	1	0	1	1
0	1	1	1	0	1
1	1	1	1	1	1

Table 2: Truth table for the controlled-SWAP gate without the Rydberg blockade.

A	B	C	A'	B'	C'
0	0	0	0	0	0
1	0	0	0	1	0
0	1	0	1	0	0
1	1	0	1	1	0
0	0	1	0	0	1
1	0	1	1	0	1
0	1	1	0	1	1
1	1	1	1	1	1

Table 3: Truth table for the controlled-SWAP gate with the Rydberg blockade.

summarized as follows:

$$1.\ |\psi\rangle_A |\phi\rangle_B |0\rangle_C \rightarrow |\psi\rangle_A |\phi\rangle_B |0\rangle_C$$

$$2.\ |\psi\rangle_A |\phi\rangle_B |1\rangle_C \rightarrow |\phi\rangle_A |\psi\rangle_B |1\rangle_C$$

However, if we were to use the Rydberg blockade, the operation that the gate performs is modified as shown below:

$$1.\ |\psi\rangle_A |\phi\rangle_B |1\rangle_C \rightarrow |\psi\rangle_A |\phi\rangle_B |1\rangle_C$$

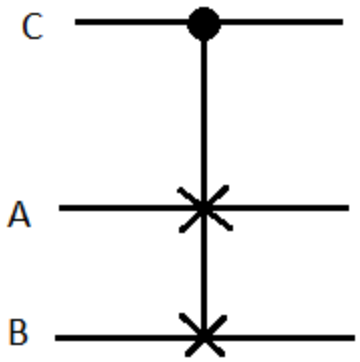

Figure 19: Circuit representation for the controlled-SWAP gate. A, B and C are the inputs, where C is the control atom and A and B are to be swapped.

$$2.\ |\psi\rangle_A |\phi\rangle_B |0\rangle_C \rightarrow |\phi\rangle_A |\psi\rangle_B |0\rangle_C$$

The behaviour of the gate is reversed from the general gate in the case of the utilization of the Rydberg blockade.

Construction: This gate can be constructed with Rydberg atoms due to the strong dipole-dipole interactions and the subsequent formation of the Rydberg blockade. The atom C plays the role of a switch, with two possible states, 0 and 1. When C is at $|1\rangle$, the SWAP operation does not take place due to the formation of the Rydberg blockade. When C is at $|0\rangle$, the Rydberg blockade is not formed and the SWAP operation occurs between A and B.

6 Conclusions and future work

Rydberg atoms, due to their large size, readily interact with other Rydberg atoms even when the separation between them is relatively large. This property of these neutral atoms is used to generate entanglement between them. The strong dipole-dipole interactions between Rydberg atoms lead to the formation of the Rydberg blockade. The blockade is realized by a shift in the energy level of the second atom in the field of the first atom and prevents the excitation of the former. This property makes Rydberg atoms a valuable tool for quantum computation, where they can act as switches.

We calculated Rabi oscillations in the case of a single atom in a system of two Rydberg atoms being irradiated by a laser. We also obtained Rabi oscillations in a system of three Rydberg atoms, in which one was the probe and the other two interacted through the dipole-dipole interaction. We concluded that the gain in entanglement and the attainment of maximum entanglement in a system is governed by the strength of the interactions between the two atoms. We finally constructed the controlled-SWAP gate, which performs the SWAP operation when the control atom is in the state $|0\rangle$, in which no blockade is formed.

As for the future work, one could place a system of two Rydberg atoms in a photon field and examine the atomic entanglement thus obtained. We predict that placing such a system in a microwave cavity will accelerate the growth of entanglement and it would peak faster. This is pertinent due to environmental decoherence, or reduction in superposition, after two Rabi oscillations.

References

[1] T. F. Gallagher, *Rydberg atoms* Vol. 3. Cambridge University Press, 2005.

[2] T. Pohl et al., *Cold and ultracold Rydberg atoms in strong magnetic fields.* Physics Reports 484.6 (2009): 181-229.

[3] G. Wunner et al., *Circular states of Rydberg atoms in strong magnetic fields.* Physical Review A 33.2 (1986): 1444.

[4] R. Löw et al., *An experimental and theoretical guide to strongly interacting Rydberg gases.* Journal of Physics B: Atomic, Molecular and Optical Physics 45.11 (2012): 113001.

[5] G. Vidal and R. F. Werner, *Computable measure of entanglement.* Physical Review A, 65(3):032314, 2002.

[6] T. A. Johnson, *Rabi oscillations and excitation blockade between ground and Rydberg states of single optically trapped rubidium atoms.* ProQuest, 2008.

[7] G. Benenti et al., *Principles of quantum computation and information: Volume I: Basic Concepts.* World scientific, 2004.

[8] M. M .Valado, *Exploring strongly correlated Rydberg excitations in cold gases using Full Counting Statistics.* PhD Thesis, University of Pisa in cotutelle with University of Heidelberg (2015).

[9] M. A. Nielsen and I. L. Chuang, *Quantum computation and quantum information.* Cambridge university press, 2010.

[10] M. Saffman et al., *Quantum information with Rydberg atoms.* Reviews of Modern Physics 82.3 (2010): 2313.

[11] M. D. Lukin et al., *Dipole blockade and quantum information processing in mesoscopic atomic ensembles.* Physical Review Letters 87.3 (2001): 037901.

[12] D. Jaksch et al., *Fast quantum gates for neutral atoms.* Physical Review Letters 85.10 (2000): 2208.

[13] D. Comparat and P. Pillet, *Dipole blockade in a cold Rydberg atomic sample.* JOSA B 27.6 (2010): A208-A232.

[14] T. J. Carroll et al., *Angular dependence of the dipole-dipole interaction in a nearly one-dimensional sample of Rydberg atoms.* Physical review letters 93.15 (2004): 153001.

[15] K. A. Smith et al., *Discrete Energy Transfer in Collisions of Xe (nf) Rydberg Atoms with NH_3 Molecules.* Physical Review Letters 40.21 (1978): 1362.

[16] E. Urban et al., *Observation of Rydberg blockade between two atoms.* Nature Physics 5.2 (2009): 110-114.

[17] A. Gatan et al., *Observation of collective excitation of two individual atoms in the Rydberg blockade regime.* Nature Physics 5.2 (2009): 115-118.

[18] M. Saffman and T. G. Walker, *Analysis of a quantum logic device based on dipole-dipole interactions of optically trapped Rydberg atoms.* Physical Review A 72.2 (2005): 022347.

[19] D. D. Yavuz et al., *Fast ground state manipulation of neutral atoms in microscopic optical traps.* Physical Review Letters 96.6 (2006): 063001.

[20] J. M. Raimond et al., *Manipulating quantum entanglement with atoms and photons in a cavity.* Reviews of Modern Physics 73.3 (2001): 565.

[21] P. McQuillen et al., *Imaging the evolution of an ultracold strontium Rydberg gas.* Physical Review A 87.1 (2013): 013407.

[22] M. Saffman and K. Mølmer, *Efficient multiparticle entanglement via asymmetric Rydberg blockade.* Physical review letters 102.24 (2009): 240502.

[23] D. Møller et al.,*Quantum gates and multiparticle entanglement by Rydberg excitation blockade and adiabatic passage.* Physical Review Letters 100.17 (2008): 170504.

[24] M. Müller et al., *Mesoscopic Rydberg gate based on electromagnetically induced transparency.* Physical Review Letters 102.17 (2009): 170502.